CORROSION SCIENCE AND TECHNOLOGY, Vol.19, No.5(2020), pp.231~238
[Research Paper]
pISSN: 1598-6462 / eISSN: 2288-6524
DOI: https://doi.org/10.14773/cst.2020.19.5.231

Comparison of Quantitative Analysis of Radioactive Corrosion Products Using an EPMA and X-ray Image Mapping

Yang Hong Jung† and Yong Sun Choo

Korea Atomic Energy Research Institute, 111 Daedeok-daero, 989 Beon-gil, Yuseong-gu, Daejeon 34057, Republic of Korea

(Received September 16, 2020; Revised October 12, 2020; Accepted October 12, 2020)

Radioactive corrosion product specimens were analyzed using an electron probe microanalyzer (EPMA) and X-ray image mapping. It is difficult to analyze the composition of radioactive corrosion products using an EPMA due to the size and rough shape of the surfaces. It is particularly challenging to analyze the composition of radioactive corrosion products in the form of piled up, small grains. However, useful results can be derived by applying a semi-quantitative analysis method using an EPMA with X-ray images. A standard-less, semi-quantitative method for wavelength dispersive spectrometry. EPMA analysis was developed with the objective of simplifying the analytical procedure required. In this study, we verified the reasonable theory of semi-quantitative analysis and observed the semi-quantitative results using a sample with a good surface condition. Based on the validated results, we analyzed highly rough-surface radioactive corrosion products and assessed their composition. Finally, the usefulness of the semi-quantitative analysis was reviewed by verifying the results of the analysis of radioactive corrosion products collected from spent nuclear fuel rods.

Keywords: *Semi-quantitative, X-ray image mapping, Shielded EPMA, Radioactive corrosion products*

1. Introduction

Electron probe micro analyzers (EPMAs) are widely applied in the analysis of chemical compositions of unknown materials, especially for irradiated nuclear fuels [1]. Quantitative analysis in EPMA analysis is usually based on a comparison of the intensities of a characteristic line emitted from a sample and from a standard of known composition. This process consists of first selecting specific lines of the elements, with the hypothesis that these elements are present in the sample, and second, measuring the X-ray intensities emitted from the unknown and the standard samples. This second step requires much time and sometimes poses problems if proper standards are not available [2,3].

Semi-Quantitative Analysis. A standard-less, semi-quantitative method for EPMA using wavelength dispersive spectrometry (WDS) was developed with a view to simplifying the analytical procedure required with this methods [4]. Based on spectrum acquisition, this method provides a way to obtain the sample composition in a short time with the advantages of the WDS system and with reasonable accuracy. To this end, three specific algorithms were designed. The first algorithm was written to automatically find all the elements present in the sample and to select the appropriate X-ray line for each element. This requires indexing automatically, with good confidence, all the peaks that are detected. The second algorithm was developed to convert the X-ray peak area from the measured spectrum into X-ray peak intensity (normally used in WDS procedures) with a Gaussian function, which is governed both by the characteristics of the WDS and by the X-ray line itself. This point is essential to prevent any under-estimation of the concentration due to the measurement of truncated peaks related to low sampling frequencies, and to improve the counting statistics by using all the information given by the spectrum. The third algorithm was written to calculate the sample composition from the absolute intensity of the selected line, and it takes into account the spectrometer efficiency. The results of the semi-quantitative analysis give, to a first approximation and in a few minutes, the sample composition. The semi-quantitative analysis is an optional procedure. It is used when the answers to a input questions are not

†Corresponding author: nyhjung@kaeri.re.kr
Yang Hong Jung: Senior Research Engineer,
Yong Sun Choo: Principal Researcher

sufficiently comprehensive or complete to allow the parameter simulation to be run [5].

Quantitative EPMA analysis entails measuring the intensity of a characteristic peak of each element present in the 'unknown' sample and comparing this with measurements on one or more standards under identical instrumental conditions. To achieve accurate quantitative analysis with WDS, it is necessary to decide which elements to include, and such a decision is based on either a qualitative spectrum, assumptions, or prior knowledge. Decisions must also be made as to which crystals to use (where wavelength coverage overlaps), background offset angles, and counting times or electron beam adjustment. As a result, experimental parameters for quantitative analysis by WDS are numerous and interdependent. The parameter settings greatly influence the quality and accuracy of the analysis results [6].

Since atmospheric particles are chemically and morphologically heterogeneous, and the average composition and the average aerodynamic diameter do not describe well the population of the particles, micro-analytical methods are necessary for their accurate study. EPMA analysis is capable of simultaneously determining the chemical composition and morphology of a single atmospheric micro particle [7,8].

2. Experimental Preparations

2.1 Specimens

Four samples were used in this study. To review the usefulness of semi-quantitative analysis methods, a fuel-cladding melting specimen with high radioactivity was prepared. This specimen offers a good surface condition for normal quantitative analysis. Samples were prepared in a hot cell, that is, a designated facility that handles highly radioactive materials. To take the macro-image of the sample for EPMA analysis, as shown in Fig. 1, the sample was mounted on a hot mounting machine and grinded using a grinding machine with grit Nos. #400 and #600, respectively, and then polished by a polishing machine with 6 um and 1 um diamond paste, respectively.

Chalk river unidentified deposit (CRUD) samples were prepared in a glove box. Paper filters with adsorbed radioactive corrosion-producing materials were cut with scissors. The cut paper filter was attached to a specimen holder using adhesive carbon tape. Because the CRUD specimens were attached to conductive carbon tape, carbon evaporation was performed for 20 seconds in consideration of electrical conductivity.

2.2 Electron probe micro analyzer (EPMA)

The shielded EPMA (JEOL JXA-8230R) used in this study was fabricated to be able to conduct highly irradiated fuels. In order to reduce the influence of radioactivity on a specimen's mounting area as well as the wavelength dispersive spectrometry (WDS) and column, the relevant parts were shielded with lead and tungsten. In addition, 15 kV and 20 nA were used for the CRUD specimens because the specimen thickness was extremely thin. The radioactive corrosion products specimens sampled from paper filter cut with scissors was attached to the specimen holder using adhesive carbon tape. Although the radioactive corrosion product specimens were attached to conductive carbon tape, carbon evaporation was performed for 10 seconds in consideration of electrical conductivity.

3. Results and Discussion

3.1 Semi-qualitative analysis

Table 1 shows the standard specimen calibration results

Table 1 (a) Standard specimen calibration results for Zr elements, and (b) the difference of coefficient results between calculated programs supplied by the EPMA manufacturer and measured using the standard specimen

Element	Zr		
Count	1st	2nd	3rd
Peak(mm)	194.568	194.564	194.554
Net(cps)	5148	5124.8	5044.5
Bg-(cps)	33.2	30.6	30.8
Bg+(cps)	18.2	22.8	19.6
S.D(%)	0.44	0.44	0.45
D.L(ppm)	436	445	434
K-raw(%)	98.585	98.691	97.467
Curr.(A)	9.99E-09	9.97E-09	9.93E-09
Intensity(cps)	5.16E+05	5.14E+05	5.08E+05

(a)

Element	Zr	Remarks
Channel	CH-3	
Crystal	PETH	
Z	40	
a	-1.97409	
b	-53.0312	
c	27.82146	
cps/100pA	52.35967	
CA(cps/uA)	523596	Caculated
ME(cps/uA)	497069	Measured
Difference	26528	CA-ME

(b)

for (a) Zr elements, and (b) the difference of coefficient results provided by the EPMA manufacturer and measured using standard specifications.

Table 1a shows the calibration values for general quantitative analysis of three sites using the Zr standard specimen. However, when the standard specimen cannot be prepared, the surface condition of the standard specimen is very rough and quantitative analysis is difficult; or when it is difficult to perform normal calibration, the coefficients for crystals provided by the manufacturer can be used.

In this study, we compared the K-raw (%), and the X-ray intensity of the standard specimen using the coefficient for crystals provided by the EPMA manufacture. The results were compared and analyzed with the values of the coefficients for crystals provided by the EPMA manufacturer. In addition, based on the results, we tried to analyze the composition of the trace-shaped radioactive corrosion products produced from spent nuclear fuel cladding. Table 1b shows the coefficients for crystals supplied by the EPMA manufacturer and the calculated results.

Coefficients for crystals supplied by the EPMA manufacturer are calculated by the equation

$$\ln(I) = a + b \times Z + c \times Z^2 + d \times Z^3 \quad (1)$$

where I = cps/100pA, Z= ln(z), z = atomic number

Table 2 compares the values of the K-raw (%) and the X-ray intensity with the K-raw (%) and the X-ray intensity of the standard specimen using coefficients for crystals provided by the manufacturer. The results are summarized and shown again. In Table 2, there is room for slight differences in each result value depending on the type of specimen and analysis conditions, but there is no significant difference. Based on this, it is judged that the values of the K-raw (%) and the X-ray intensity using coefficients for crystals provided by the manufacturer can be used as basic data for quantitative analysis. This can have the justification of basic data for quantitative analysis for the following reasons. If the population is known to be normal, the sampling distribution of will follow a normal distribution exactly, no matter how small the size of the samples [9]. Thus, the confidence interval for μ is calculated by the equation

$$\bar{x} - z_{\alpha/2}\frac{\sigma}{\sqrt{n}} < \mu < \bar{x} + z_{\alpha/2}\frac{\sigma}{\sqrt{n}} \quad (2)$$

, where

$$Z = \frac{\bar{X} - \mu}{\sigma/\sqrt{n}}, \qquad P\left(-z_{\alpha/2} < Z < z_{\alpha/2}\right) = 1 - \alpha$$

From equation (2), the confidence interval, (1-α) 100%, of the difference between calculated and measured X-ray intensities (cps/uA) is within 97.36%.

The K-raw (%) values are almost identical between Table 1 and Table 2, so the K-raw (%) in Table 1 is calculated by a program developed by the EPMA manufacturer considering the confidence interval with difference between calculated and measured X-ray intensity (cps/uA) for Zr. Therefore, in the case of testing the quantitative analysis for an unknown specimen without standard specimens, it is feasible for the analysis results can be reflected by the semi-quantitative analysis [10].

A semi-quantitative analysis of radioactive corrosion products is attempted based on the data presented in Table 1 and Table 2. As already explained, the surface of radioactive corrosive products is not only rough but also not flat, making it difficult to perform quantitative analysis with an EPMA. Therefore, first, we selected a well-prepared sample and compared the results of the calculated program supplied by the EPMA manufacturer and calculation by adapting the probability and statistics. If the result of weight (%) obtained here proved satisfactory, the samples of radioactive corrosive products could be analyzed. Fig. 1 shows the irradiated U-Zr–based fuses and ferritic-martensitic stainless steel cladding. The data shown in Fig. 1 have been condensed as the most possible fuel for the initial core of a sodium-cooled fast reactor [11].

Table 2 Comparison of intensity and K-raw (%) between the calculated program supplied by the EPMA manufacturer and the calculation by adapting the probability and statistics

Element	JEOL Cal_STD			Cal_ probablity and statistics			Ave.	
Frequency	1st	2nd	3rd	1st	2nd	3rd	**Cal_STD**	**Cal_pro**
Intensity	5.16E+05	5.14E+05	5.08E+05	5.14E+05	5.13E+05	5.07E+05	5.13E+05	5.11E+05
K-raw(%)	98.96	98.69	97.47	97.95	97.68	96.46	**98.37**	**97.36**

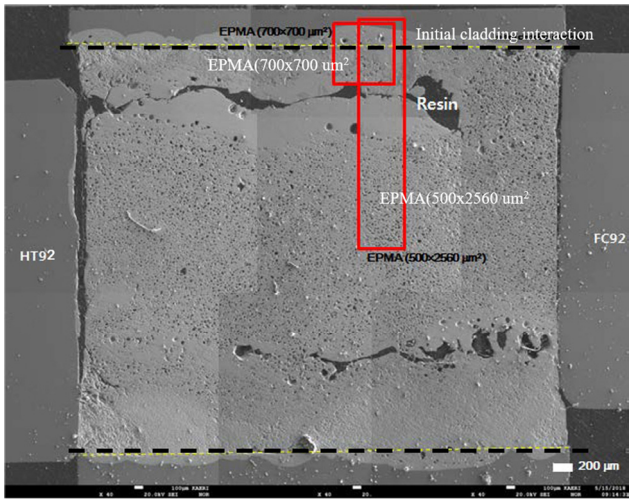

Fig. 1 SEM image of the cross-section of the radial-axial plane of the irradiated fuel specimen.

Table 3 Comparison of Fe composition for the HT9 materials with and without standard specimens

Items	HT9 tube	Standard	Standard-less
Fe wt%	85.82	85.3	82.24

The fuel rod of U-10Zr with T92 cladding was irradiated in the HANARO test reactor at Korea Atomic Energy Research Institute. The fuel rods were irradiated for 182 effective full-power days [12].

Fig. 1 shows the cross-section of the radial-axial plane of the specimen. The black dashed line represents the initial fuel-cladding boundary, and the red dashed line represents a significant fuel-cladding interface occurring uniformly along the cladding materials of HT92. Table 3 shows the formation of clad materials (HT9). Fig. 2 shows the results of the analysis of the red dashed line in Fig. 1. In the scanning electron microscopy (SEM) image in Fig. 2, the cladding materials, HT92, and the fuel rod of U-10Zr can be found to be fused together. Observing the X-ray image mapping of cladding materials (HT92) (whose iron composition is 85.82 wt%, as shown in Table 3) yields a qualitative observation of the shape of the solidified metal tissues after the melting of the cladding and fuel, as shown in Fig. 2. It is impossible to analyze the composition of molten tissue with various shapes using an EPMA, as shown in Fig. 2.

As shown in Table 3, the composition of Fe measured using the standard specimen at the cladding material location of Fig. 2 was 85.3 wt%. In addition, as shown in Table 3, the composition of Fe measured by the semi-quantitative analysis method without a standard specimen was confirmed to be 82.24 wt%. This is a comparison of the analysis results for only one point, and it is considered that it confirms an acceptable result. The

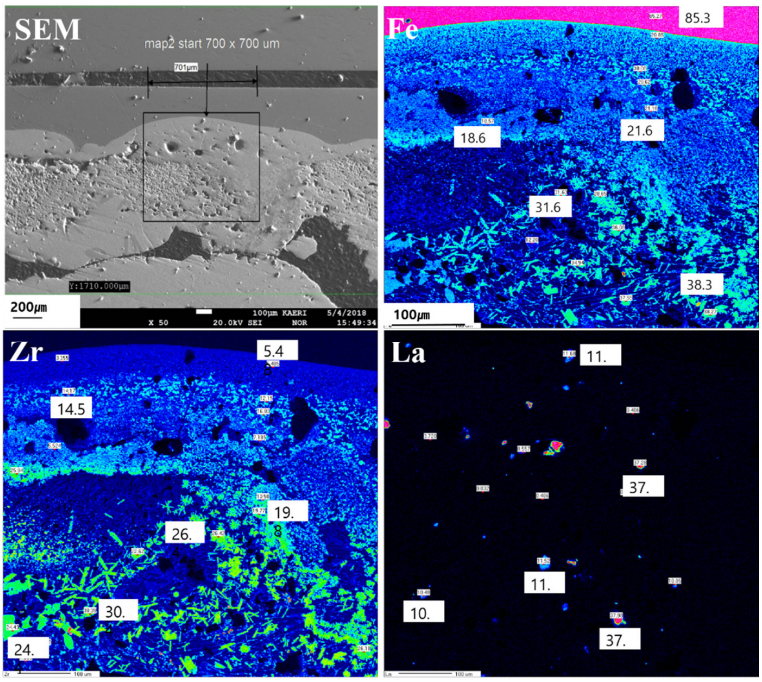

Fig. 2 SEM image of pellet-cladding interaction in the irradiated fuel rod, and X-ray image mapping of Fe, Zr, and La elements.

analysis results shown in Table 3 were preliminary tests to verify the usefulness of the semi-quantitative analysis method used in this study. That is why the analysis of one point was performed and the results were accepted.

As shown in Fig. 2, the quantitative analysis values of Fe, Zr, and La are the compositions confirmed by the semi-quantitative analysis method. As can be seen in Fig. 2, the excellent feature of the semi-quantitative analysis method is that it is possible to confirm the composition of a specific area while observing the shape of the sample confirmed by X-ray image mapping as a picture.

Based on the semi-quantitative analysis method verified in Fig. 2, the analysis of radioactive corrosion products was performed, as shown in Fig.s 3, 4, and 5.

The CRUD specimens shown in Fig. 3 are several tens of micrometer in size, and the roughness of the surface is also very rough, as shown in the figure [13]. The data analyzed by EPMA analysis using a standard specimen are shown at the bottom of the figure. Due to the surface roughness of the sample, the overall average composition for the three points was about 53 wt%.

This analysis method is not appropriate because it is a method of analyzing after checking the surface condition of a sample with SEM images. However, as shown in

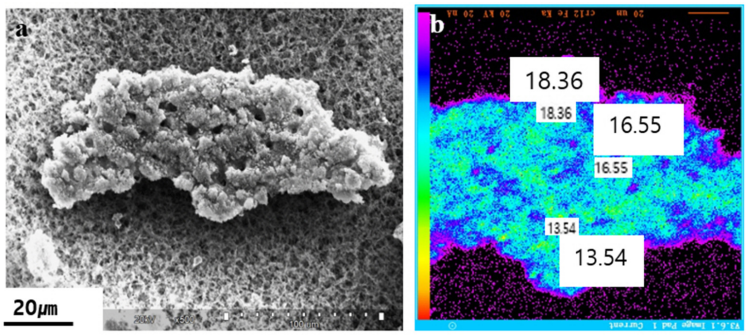

Item	Fe	Ni	Cr	Zn	O	Total
1	14.62	28.63	2.15	0.93	12.51	58.84
2	17.60	22.73	1.83	0.72	10.24	53.13
3	15.95	19.63	2.04	0.65	9.49	47.76
Ave	16.06	23.66	2.01	0.77	10.75	53.24

Fig. 3 SEM and X-ray image mapping of Fe in the radioactive CRUD flake specimen.

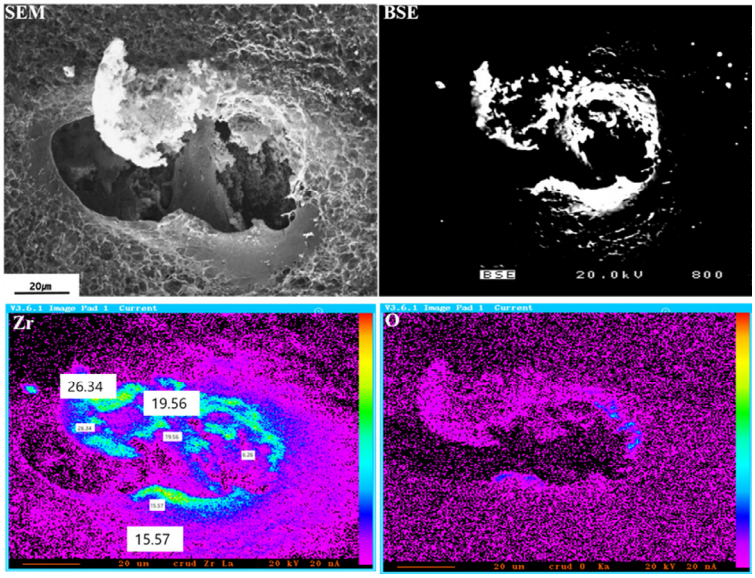

Fig. 4 SEM, BSE, and X-ray image mapping of Zr and O elements on the smear filter paper of the CRUD specimen.

Fig. 3b, it is determined to be a usable analysis method because the semi-quantitative result values for the desired site are checked with the identification of specific parts and shapes of samples identified by X-ray image mapping. Rather than analyzing the composition while observing the surface of the sample with SEM, as shown in Fig. 3b, there is the convenience of checking the composition by simply clicking the desired point while viewing the X-ray image mapping. Of course, it was confirmed that the semi-quantitative analysis result has an acceptable value, as shown in Fig. 2. In Fig. 3, the composition of Fe analyzed using the standard specimen was 16.06 wt%. In addition, it was confirmed that the composition of Fe analyzed by the semi-quantitative method had a useful value of 16.15 wt%.

Fig. 4 shows the shape of the CRUD specimens attached to the paper filter after being melted using an electron beam [13, 14]. As shown in Fig. 4, it is difficult to confirm the composition of the sample when the location of the element to be analyzed is not visible or the existence itself is incorrect. However, if the semi-quantitative analysis method shown in Fig. 4 is used, it becomes a useful method to confirm the existence shape and proper composition of the sample, as shown in the images. In fact, when the need to confirm the composition of a material having such a shape comes to the fore, when analyzing the composition of a sample using EPMA analysis, it should be recognized that the only method of analysis is a semi-quantitative method. Again, the semi-quantitative method is a useful method for radioactive corrosion products with severe sur-

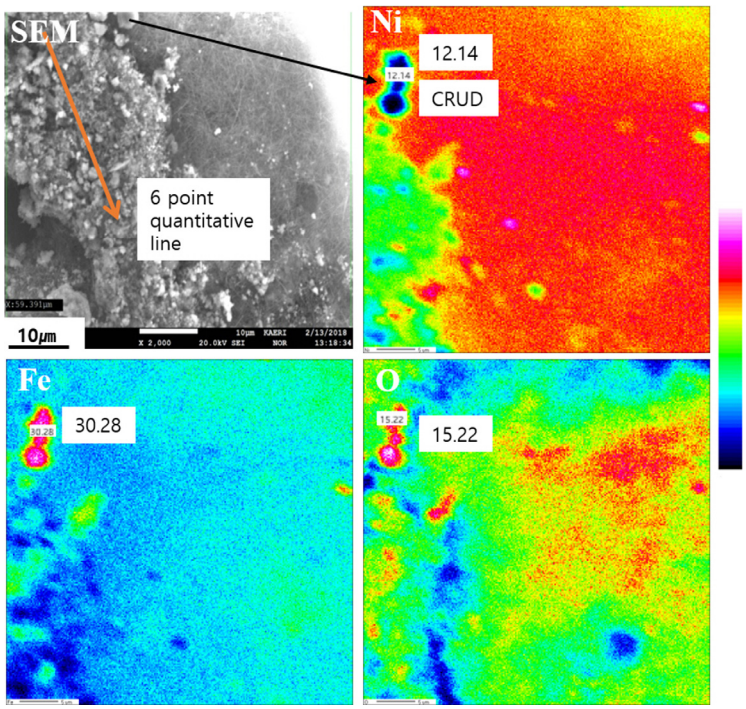

Fig. 5 SEM of a CRUD flake sampled with ultrasonic cleaner in a pressurized water reactor plant, and X-ray image mapping of Ni, Fe, O.

Table 4 The 6-point quantitative analysis results of a CRUD flake as shown in Fig. 5(wt%)

Ele.	Ni	O	Si	Fe	Cr	Zr
1	7.82	11.43	2.03	7.51	1.94	0.27
2	11.90	10.30	4.38	11.29	3.12	0.00
3	12.69	9.15	5.16	9.21	2.80	0.00
4	5.70	8.70	1.83	8.02	1.74	0.00
5	7.30	7.23	5.17	9.42	2.88	0.00
6	9.31	7.09	1.19	6.29	0.64	3.47
Ave.	9.12	8.98	3.29	8.62	2.19	0.62

face roughness.

Fig. 5 shows the SEM shape of typical corrosive products bonded to nuclear fuel cladding and the result of Ni, Fe, and O X-ray image mapping. In the figure, among the corrosive products of various forms of debris, the existence of CRUD, which nuclear power plant workers and researchers are interested in, was identified. Table 4 shows the results of quantitative analysis using the standard specimen for six sections of radioactive corrosion products at random, as shown in Fig. 5. The analysis results in Table 4 reveal 9.12 wt% Ni, 8.62 wt% Fe, and 8.98 wt% O. The results of this were not identified as the chemical composition of the CRUD, $NiFe_2O_3.x$ (18.65 wt% Ni, 32.45 wt% Fe, and 17.68 wt% O).

In other words, the corrosive products identified in Table 4 could be considered as general corrosive materials, not CRUD materials. However, in the X-ray image mapping of Fig. 5, the analysis of the unusually observed masses by the semi-quantitative analysis method showed that 12.14 wt% Ni, 30.28 wt% Fe, and 15.22 wt% O were identified. This value represents a result similar to $NiFe_2O_3.x$, which is the main element chemical formula of CRUD. In other words, the mass identified in Fig. 5 was determined to be CRUD. In fact, when the need to confirm the composition of a material having such a shape comes to nuclear power plants, when analyzing the composition of a sample using an EPMA, it should be recognized that the only method of analysis is a semi-quantitative method. Again, the semi-quantitative method is a useful method for radioactive corrosion products with severe surface roughness.

4. Conclusions

Radioactive corrosion product specimens were analyzed using an electron probe micro analyzer (EPMA) and X-ray image mapping. Semi-quantitative analysis and observation of the semi-quantitative results using a good surface condition sample were conducted. The values of the K-raw (%) and the X-ray intensity of the standard specimen using coefficients for crystals provided by the EPMA manufacturer were compared. There is room for slight differences in each result value depending on the type of specimen and analysis conditions, but there is no significant difference.

Observing the X-ray image mapping of cladding materials (HT92), the composition of Fe measured by the semi-quantitative analysis method without a standard specimen was confirmed to be 82.24 wt%. It is considered that it confirms an acceptable result. Based on the validated results, we analyzed the highly rough-surface radioactive corrosion products and reviewed their composition. Finally, the usefulness of semi-quantitative analysis can be reviewed by verifying the analysis results of radioactive corrosion products collected from spent nuclear fuel rods. In fact, when nuclear power plants have the need to confirm the composition of a material having such an irregular shape, when analyzing the composition of a sample using an EPMA, it should be recognized that the only method of analysis is a semi-quantitative method. Again, the semi-quantitative method is a useful method for radioactive corrosion products with severe surface roughness.

References

1. S. Bremier, K. Inagaki, L. Capriotti, P. Poeml, T. Ogata, H. Ohta, and V. V. Rondinella, *J. Nuc. Mat.*, **480**, 109 (2016). https://doi.org/10.1016/j.jnucmat.2016.07.060
2. C. Fournier, C. Merlet, O. Dugne, and M. Fialin, *J. Anal. At. Spectrom.*, **14**, 381 (1999). https://doi.org/10.1039/A807433J
3. R. A. Barrea and R. T. Mainardi, *X-ray Spectrom.*, **27**, 111 (1998). https://doi.org/10.1002/(SICI)1097-4539(199803/04)27:2<111::AID-XRS259>3.0.CO;2-3
4. C. Fournier, C. Merlet, M. Fialin, and O. Duhne, *J. Anal. At. Spectom.*, **14**, 381 (1999). https://doi.org/10.1039/A807433J
5. C. Fournier, C. Merlet, P. F. Staub, O. Dugne, *Microchim. Acta*, **132**, 531 (2000). https://doi.org/10.1007/s006040050105
6. S. J. B. Reed, *Microchim. Acta (Suppl.)*, **15**, 29 (1998). https://doi.org/10.1007/978-3-7091-7506-4_4
7. J. Osán, Sz. Török, K. Török, L. Németh, and J. L. Lábár, *X-Ray Spectrom.*, **25**, 167 (1996).
8. W. Jambers and R. Van Grieken, *Environ. Sci. Technol.*,, **31**, 1525 (1997). https://doi.org/10.1021/es9608003
9. R. E. Walpole and R. H. Myers, probability and statistics for engineers and scientists, *3rd ed.*, p. 182 - 193, Macmillan, USA (1985).
10. Y. S. Choo, Y. J. Kim, B. O. Yoo, S. J. Baik, Y. G. Jin, K. S. Heo, H. M. Kim and S. B. Ahn, *Proc. KNS 2017 Autumn Meeting*, Gyeongju, Korea (2017). https://www.kns.org/files/pre_paper/38/17A-569%EC%A3%BC%EC%9A%A9%EC%84%A0.pdf
11. J.-S. Kim, J. -H. Kim, B. -O. Lee, Y. -H. Jung, B. -O. Yoo, Y. -J. Kim, and J. -S. Cheon, *Proc. KNS 2018 Autumn Meeting*, Yeosu, Korea (2018). https://www.kns.org/files/pre_paper/40/18A-145%EA%B9%80%EC%A3%BC%EC%84%B1.pdf

12. J.-H. Kim, J.-S. Cheon, B.-O. Lee, J.-H. Kim, H.-M. Kim, B.-O. Yoo, Y.-H. Jung, S.-B. Ahn, and C.-B. Lee, *Met. Mater. Int.*, **23**, 504 (2017). https://doi.org/10.1007/s12540-017-6515-1
13. Y. H Jung, S. J, Baik, and S. B, Ahn, *Corros. Sci. Tech.*, **17**, 265 (2018). https://doi.org/10.14773/cst.2018.17.6.265
14. J. C. Deshon, S. T. Yang, Y. H Jung, and J. C. Shin, Zinc Injection Program Assessment of Ulchin-1, pp. 70 - 75, EPRI final report, August (2011).